

Identifying osteosarcoma metastasis associated genes by weighted gene co-expression network analysis (WGCNA)

Honglai Tian, MD^{a,*}, Donghui Guan, MD^a, Jianmin Li, MD^{b,*}

Abstract

Osteosarcoma (OS), the most common malignant bone tumor, accounts for the heavy healthy threat in the period of children and adolescents. OS occurrence usually correlates with early metastasis and high death rate. This study aimed to better understand the mechanism of OS metastasis.

Based on Gene Expression Omnibus (GEO) database, we downloaded 4 expression profile data sets associated with OS metastasis, and selected differential expressed genes. Weighted gene co-expression network analysis (WGCNA) approach allowed us to investigate the most OS metastasis-correlated module. Gene Ontology functional and Kyoto Encyclopedia of Genes and Genomes (KEGG) pathway enrichment analyses were used to give annotation of selected OS metastasis-associated genes.

We select 897 differential expressed genes from OS metastasis and OS non-metastasis groups. Based on these selected genes, WGCNA further explored 142 genes included in the most OS metastasis-correlated module. Gene Ontology functional and KEGG pathway enrichment analyses showed that significantly OS metastasis-associated genes were involved in pathway correlated with insulin-like growth factor binding.

Our research figured out several potential molecules participating in metastasis process and factors acting as biomarker. With this study, we could better explore the mechanism of OS metastasis and further discover more therapy targets.

Abbreviations: DEGs = differentially expressed genes, FDR = false discovery rate, GEO = Gene Expression Omnibus, GO = gene ontology, GS = gene significance, *IGFBP5* = insulin-like growth factor binding protein 5, *IGFBP6* = insulin-like growth factor binding protein 6, IGFBPs = insulin-like growth factor binding proteins, *KAI-1* = kangai1, KEGG = Kyoto Encyclopedia of Genes and Genomes, MAPK = mitogen-activated protein kinase, *MKK4* = mitogen-activated protein kinase 4, *MMP11* = matrix metalloproteinase 11, *MYL2* = myosin light chain 2, *NOV* = nephroblastoma overexpressed, NPV = negative predictive value, OS = osteosarcoma, PPV = positive predictive value, RFE = recursive feature elimination, ROC = receiver operating characteristic curve, Se = sensitivity, Sp = specificity, SVM = support vector machines, *WISP3* = WNT1 inducible signaling pathway protein 3.

Keywords: metastasis, osteosarcoma, weighted gene co-expression network analysis

1. Introduction

Osteosarcoma (OS) is the most common primary malignant bone tumor in childhood and adolescence. OS exhibits highly

aggressive and early systemic metastasis.^[1,2] About 20% of OS patients appear focus metastasis when they receive the first diagnosis. With the great development of effective chemotherapy combinations, the survival rates of nonmetastatic OS have significantly increased from <20% before 1970s to present rates of 65% to 75%.^[3,4] However, OS systemic metastasis, especially the occurrence of lung metastasis is still the most prominent reason for OS-caused death. Only 11% to 30% of patients suffering from OS metastasis can survive after the combination of surgery resection and chemotherapy.^[5,6] In this way, OS metastasis has become the obstacle for successful OS treatments. OS metastasis is a multistep dynamic progression facilitated by pro-metastasis genes such as *myc*,^[7] *ras*,^[8] and inhibited by metastasis-resistant genes including *nm23*,^[9] *p16*,^[10] *kangai1* (*KAI-1*),^[11] *KiSS-1* metastasis-suppressor (*KISS-1*),^[12] mitogen-activated protein kinase 4 (*MKK4*). Although the biological characteristic of OS has been understood a lot, a large scale of regions in molecular mechanisms involved in OS metastasis are still uncovered. Therefore, in order to profoundly improve early diagnostic efficacy and clinical outcomes for patients with OS, it is not only urgent to find out the metastasis mechanism but also to identify molecular that can be used as candidate diagnostic biomarkers or therapeutic targets in OS.

Bioinformatic approaches are increasingly being used in target genes or proteins exploration and analysis. Weighted gene co-expression network analysis (WGCNA) is a novel gene co-expression network-based approach. WGCNA is a systems

Editor: Jianxun Ding.

HT and DG should be regarded as co-first authors.

Ethics committee: This is a meta-analysis manuscript, there is no ethics committee or institutional review board approved by the study.

Competing interests: The authors declare that they have no competing interests.

Supplemental Digital Content is available for this article.

^a Department of Orthopaedics, Affiliated Hospital of Shandong University of Traditional Chinese Medicine, ^b Department of Orthopaedics, Qilu Hospital of Shandong University, Wenhua West Road, Jinan City, Shandong, China.

* Correspondence: Honglai Tian, Department of Orthopaedics, Affiliated Hospital of Shandong University of Traditional Chinese Medicine, No. 16369 Jingshi Road, Lixia District, Jinan City, Shandong, China (e-mail: tianh lai@163.com), Jianmin Li, Department of Orthopaedics, Qilu Hospital of Shandong University, No. 42 Wenhua West Road, Jinan City, Shandong 250012, China (e-mail: gkijm@163.com).

Copyright © 2018 the Author(s). Published by Wolters Kluwer Health, Inc. This is an open access article distributed under the terms of the Creative Commons Attribution-Non Commercial-No Derivatives License 4.0 (CCBY-NC-ND), where it is permissible to download and share the work provided it is properly cited. The work cannot be changed in any way or used commercially without permission from the journal.

Medicine (2018) 97:24(e10781)

Received: 17 July 2017 / Accepted: 24 April 2018

<http://dx.doi.org/10.1097/MD.00000000000010781>

biology method for molecular interaction mechanism analysis and correlation networks resolving.^[13] In accordance with high throughput microarray data, WGCNA can be used to seek synergetic expressed modules and explore the relationship between gene networks and clinical phenotype at transcriptome level.^[13–15] As an effective and accurate bioinformatics method, WGCNA has been widely applied in identifying susceptibility genes, screening candidate targets for disease and cancer fields.^[16,17] In 2017, Liu et al^[18] predict gene clusters correlated with the mechanisms of OS using WGCNA, finding that the genes in module 5 are involved in OS. However, the pathogenesis of OS has not been fully revealed.

Previous studies offered a series of Gene Expression Omnibus (GEO) datasets presenting OS related genes expression profile. These analyses comprise bioinformatics data derived from tissue sample of OS patients. In this study, we selected some of these dataset with specific limitation for our bioinformatics analysis.^[19–21] We conducted WGCNA and the following support vector machines (SVM) to analyze OS metastasis related genes and identified key genes potentially participated in OS metastasis progression. With the usage of effective bioinformatic analysis, we can figure out specific key genes that have important clinical implications in disease basic researches and clinical therapy.

2. Methods

2.1. Data collection and preprocessing

Four expression profile data sets of OS metastasis were downloaded from the GEO database (<https://www.ncbi.nlm.nih.gov/gds>). Datasets GSE14359, GSE21257, GSE32981, and GSE14827 were chosen for further study in accordance with the following rules: datasets belong to OS gene expression profiles; datasets contain OS metastasis and nonmetastasis classification information. GSE14359 dataset was used for OS significantly correlated modules and genes selection, and SVM establishment. The other three datasets were used for independent verification of SVM. Detail information of datasets was shown in Table 1. GSE14359 and GSE14827 data sets in GEL format were annotated according to the Affymetrix Human Genome U133A and U133 Plus 2.0 Array platforms respectively. The background correction and normalization of these raw data sets were performed by the Affy^[22] package in R. GSE32981 was derived from ABI Human Genome Survey Microarray v2.0 platform. GSE21257 was obtained from Illumina^[23] human-6 v2.0 expression beadchip (using nuIDs as identifier). GSE32981 and GSE21257 datasets were downloaded in original txt format.

Probes were mapped to gene symbols. Empty probes were discarded according to the annotation platform of each expression profiles. If there were multiple probes that mapped to the same gene symbol, their mean value was considered as the gene expression value. Data were normalized by the limma (linear models for microarray data) package in R.

2.2. Screening for differentially expressed genes

The differentially expressed genes (DEGs) between nonmetastasis and metastasis group in GSE14359 were screened by the limma package in R. The adjusted *P*-value (false discovery rate, FDR) $<.05$ and $|\log FC| > 1$ were set as the cut-off criteria.

2.3. Screening for OS associated genes and modules by WGCNA

Module identification was accomplished with the dynamic tree cut method. Highly similar modules were identified by cluster analysis and then merged together with a height cut-off of 0.95. For further quantification of OS related genes and modules, the *p*-value of gene expression difference between normal group and disease group were evaluated with T-test, and $\log P$ was considered as gene significance. The mean value of gene significance (GS) derived from modules comprising gene was defined as module significance.

2.4. Establishment of SVM

GSE14539 was set as training dataset. The genes feature combination was obtained through recursive feature elimination (RFE) arithmetic. SVM was established with the selected optimized gene feature combination. To test the stability and transferability of SVM, the generated SVM was verified by using independent test datasets: GSE14827, GSE21257, and GSE32981. The classification effect was determined according to sensitivity (Se), specificity (Sp), positive predictive value (PPV), negative predictive value (NPV), and proportion under Receiver operating characteristic curve (ROC) curve.

3. Results

3.1. Datasets preprocessing and DEGs selection

In order to select OS metastasis associated genes, datasets about OS associated gene expression profiles were downloaded from the GEO Database (see Methods and Fig. 1 for details on the experimental design).

Under the thresholds of $|\log FC| > 1$ and $FDR < 0.05$, total 897 DEGs were obtained from GSE14359 dataset. Bidirectional hierarchical clustering was carried out according to the genes expression level and the results were presented by the heat map exhibiting genes mRNA expression level (Fig. 2).

3.2. Dataset network construction and modules detection

In order to identify OS-metastasis associated modules and genes, WGCNA was performed on the obtained 897 DEGs. Firstly, we explored the value of adjacency matrix weighting, power. As shown in Figure 3, X-axis represents matrix weighting power while the Y-axis represents quadratic correlation index derived

Table 1
Datasets of gene expression profiles.

GEO accession	Platform	Probe number	Total sample number	Metastasis	Nonmetastasis
GSE32981	GPL3307	14725	23	18	5
GSE21257	GPL10295	48701	53	34	19
GSE14359	GPL96	22283	18	8	10
GSE14827	GPL570	42450	27	9	18

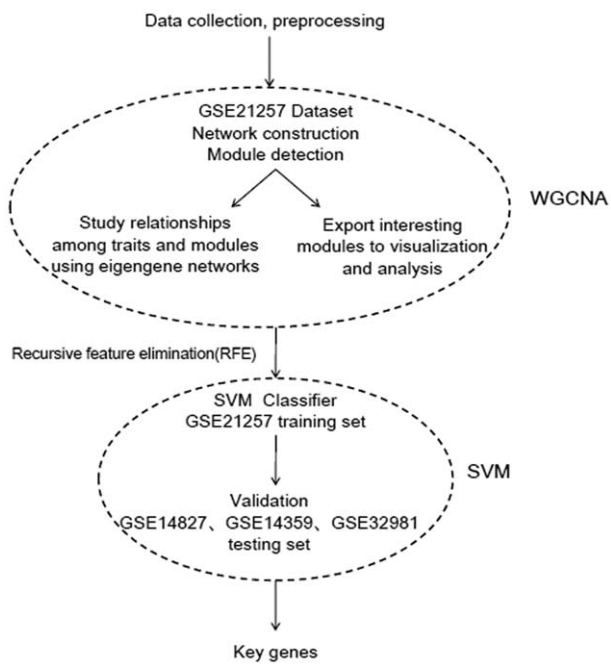


Figure 1. The workflow of data preparation, processing, analysis, and validation in this study.

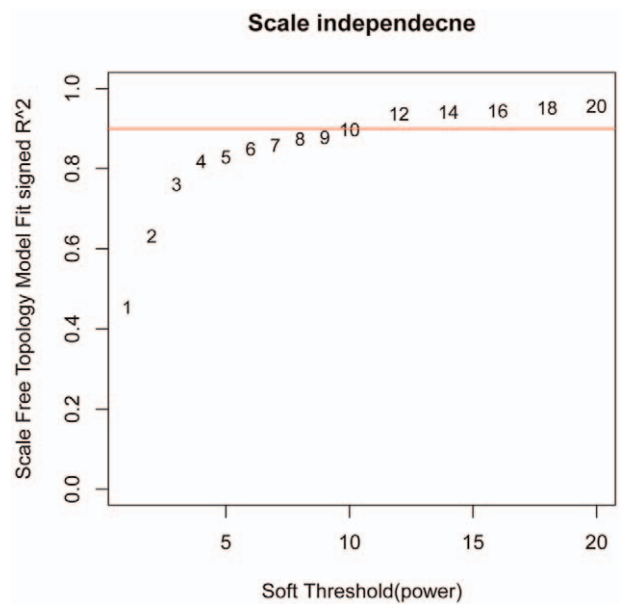


Figure 3. Calculation chart of adjacency matrix weighting parameters (power). The X-axis represents weighting parameters (power). The Y-axis represents quadratic of correlation index from $\log(k)$ and $\log(P(k))$.

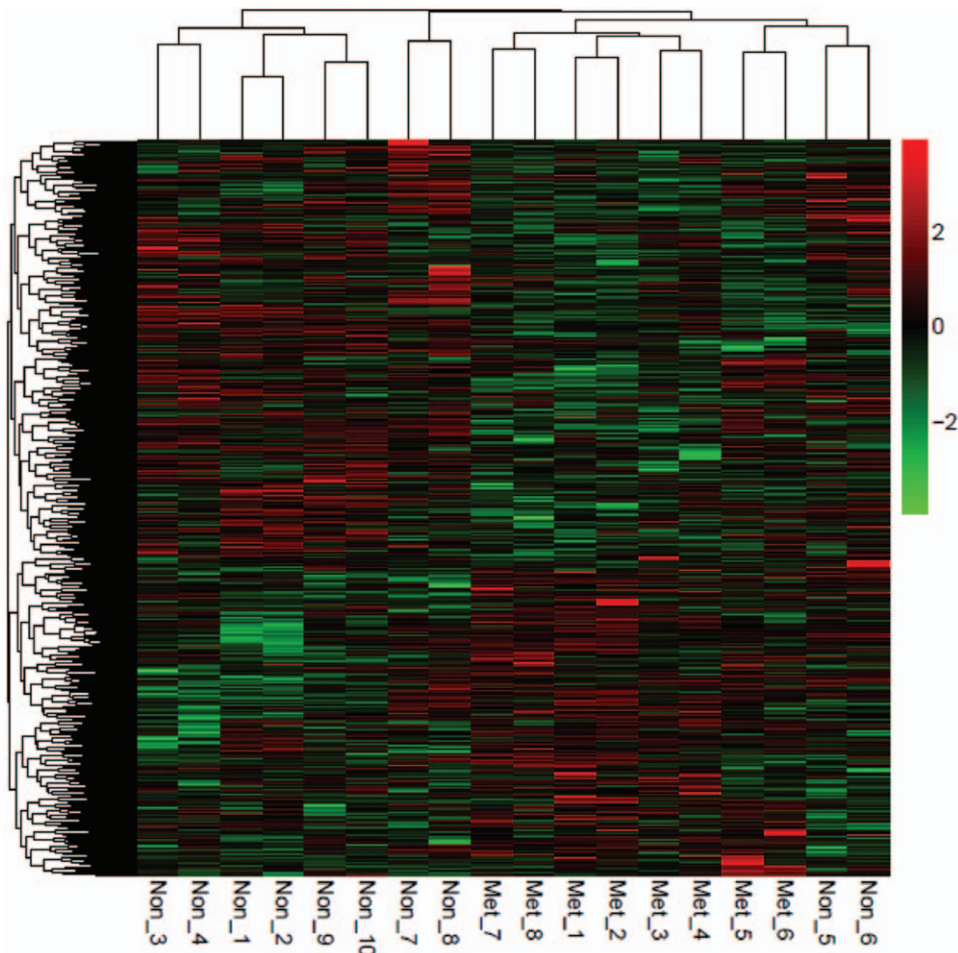


Figure 2. Heat map of the difference of genes mRNA expression in GSE14359. Red color exhibits upregulated genes while the green means the downregulated genes. The correlation between color and the fold change of genes mRNA level is displayed in the upper right.

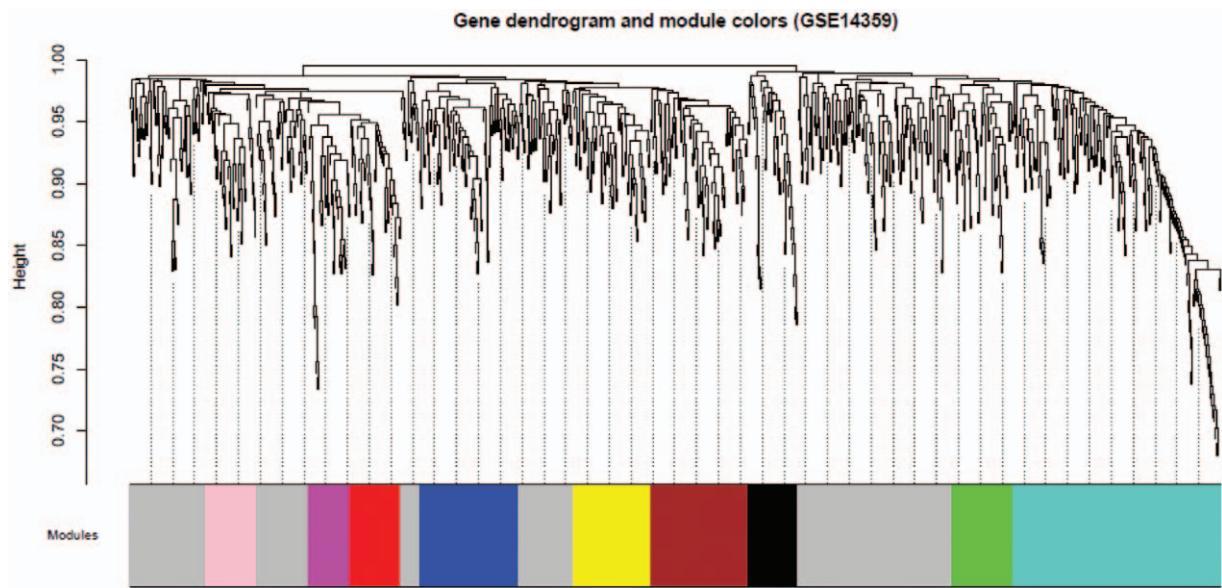


Figure 4. Clustering dendrograms of GSE14359. System clustering tree was built based on GSE14359 dataset. Ten kinds of color present 10 modules.

from $\log(k)$ and $\log(P(k))$ of the corresponding network. From Figure 3, we took power as 12 when correlation index reached 0.9 the first time.

In the next step, we calculated community dissimilarity index of DEGs and obtained system clustering tree. According to the standard of dynamic cut tree, we set 30 as the least gene number of each gene network and 0.95 as the cut-height, respectively. After determination of gene modules by using dynamic tree cut method, we computed the eigenvector value of each module. Based on cluster analysis of modules, the closer ones were merged together for new modules' acquisition. Modules partition was shown in Figure 4, we totally obtained 10 osteosarcoma-metastasis associated modules.

In further, we qualified the relevance between eigenvalue of network modules and osteosarcoma-metastasis condition (me-

tastasis and nonmetastasis). As shown in Figure 5, gene significance of each modules were over 0.8 while modules significance P -value was only .0072, far lower than 0.05, indicating significant difference among modules. The specific DEGs in obtained 10 modules were recorded in Table S1, <http://links.lww.com/MD/C291>. The turquoise pattern contained the largest number of DEGs among these modules. So we took DEGs in this module for further study.

3.3. Generation and annotation of OS associated module network

We established genes expression network by using OS associated gene expression value from turquoise panel. As shown in Figure 6, the network contains 231 connection sides

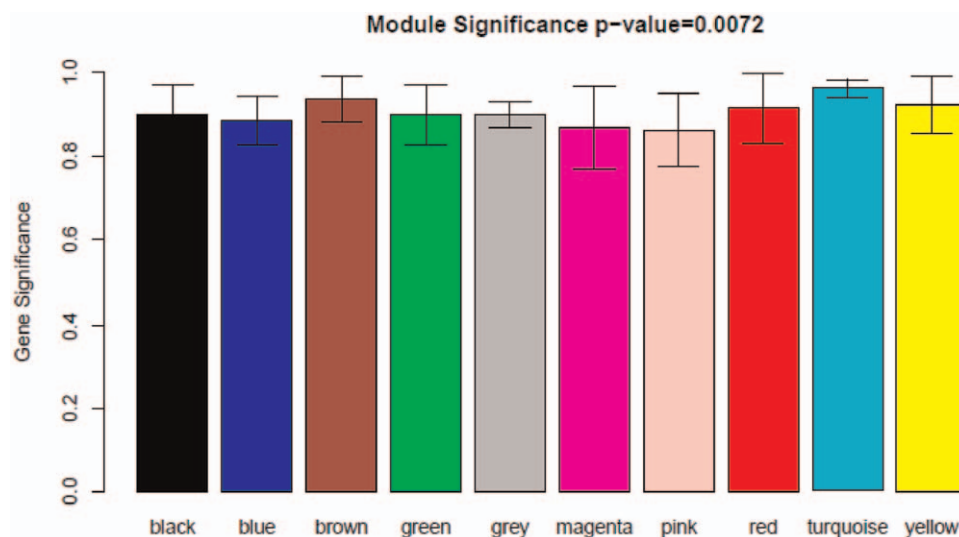


Figure 5. Diagram of correlation of module's color and osteosarcoma. The relevance between eigenvalue of network modules and osteosarcoma-metastasis condition was qualified. The colored row indicates modules and the Y-axis represents gene significance.

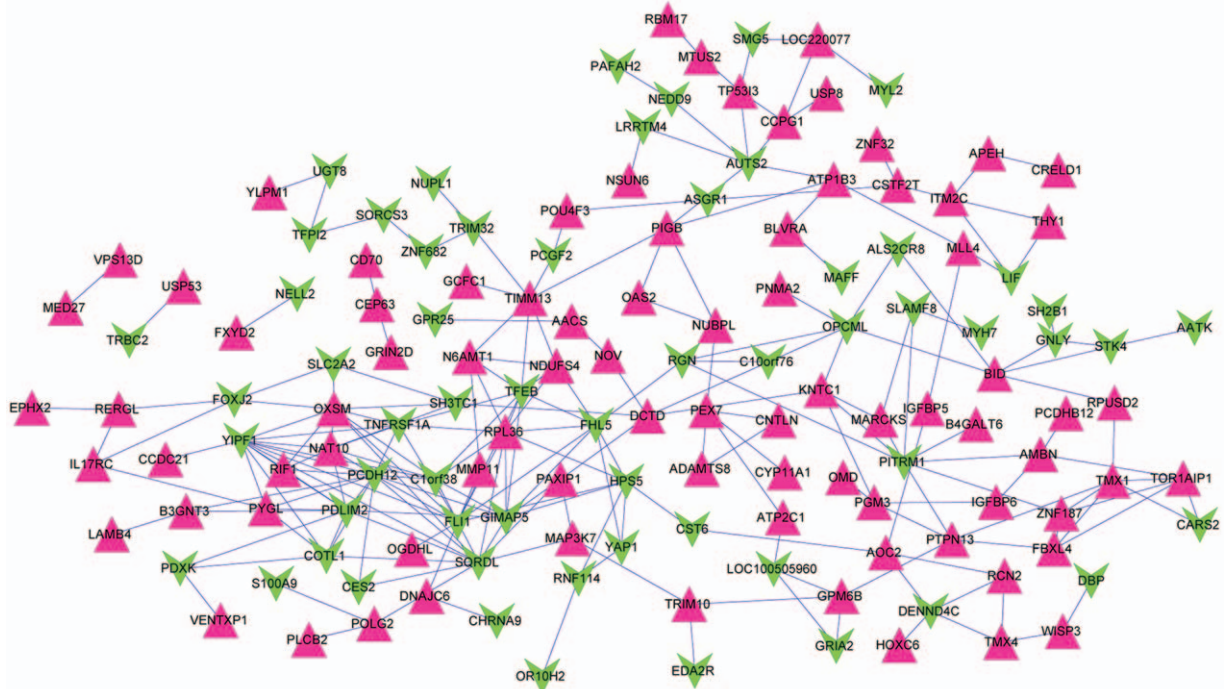


Figure 6. Gene expression network derived from turquoise module. Equilateral triangle and inverted triangle represent downregulation and upregulation, respectively. The red point meant significantly upregulated expression genes while the green point meant down-regulated expression genes.

and 142 nodes comprising 59 downregulated genes and 83 upregulated genes. All these 142 genes were subjected to Gene Ontology (GO) functional and Kyoto Encyclopedia of Genes and Genomes (KEGG) pathway enrichment analyses and the annotations were presented in Figure 7 and Table 2. As shown in Table 2, nephroblastoma overexpressed (*NOV*), insulin-like growth factor binding protein 5 (*IGFBP5*), insulin-like growth factor binding protein 6 (*IGFBP6*), WNT1 inducible signaling pathway protein 3 (*WISP3*) and myosin light chain 2 (*MYL2*) were found in both cell growth regulation and insulin-like growth factor binding groups. These data indicated that these genes and associated functional pathway may contribute to the progression of tumor cell migration.

3.4. Optimal characterized genes selection

To confirm typical characterized genes involved in these 142 genes, we chose GSE14359 as training dataset and conducted feature selection with recursive feature elimination (RFE). If there were 12 genes combination, 17 samples were accurately classified with accuracy rate of 94.4% (Fig. 8). All these 12 genes, especial tumor-associated gene matrix metalloproteinase11 (*MMP11*), FXYP domain containing ion transport regulator 2 (*FXYP2*) were presented in Table 3.

3.5. Verification and assessment of SVM

GSE14827, GSE21257, and GSE32981 datasets were utilized to verify the SVM generated by the selected optimized gene feature

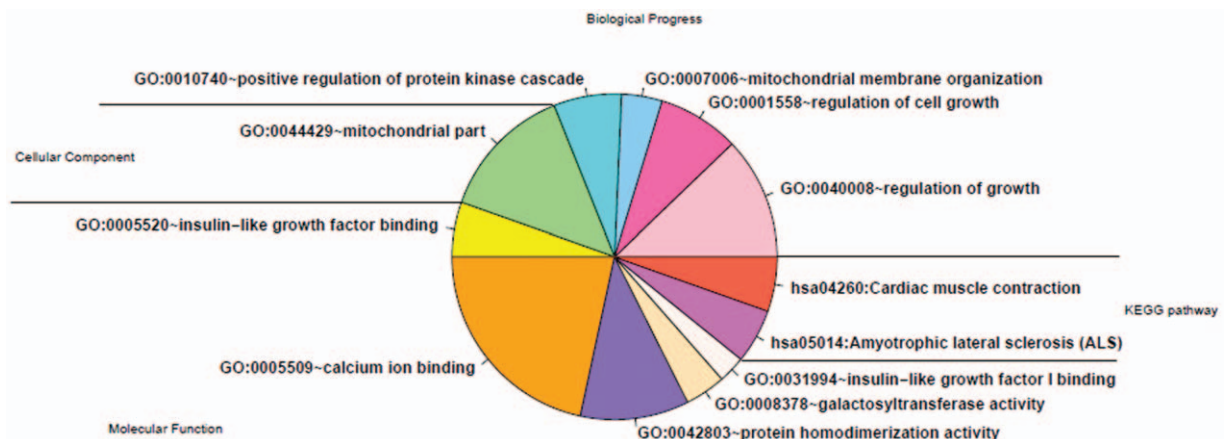


Figure 7. Annotation of KEGG pathway enrichment analysis and gene ontology function of differentially expressed genes. KEGG= Kyoto Encyclopedia of Genes and Genomes.

Table 2
Annotation of KEGG pathway enrichment analysis and gene ontology function of differentially expressed genes list.

Term	Count	P value	Genes
GO:0040008—regulation of growth	9	.007374	NOV, TMX1, MYL2, WISP3, IGFBP6, NELL2, NEDD9, N6AMT1, IGFBP5
GO:0001558—regulation of cell growth	6	.022527	NOV, MYL2, WISP3, IGFBP6, N6AMT1, IGFBP5
GO:0007006—mitochondrial membrane organization	3	.028669	BID, GIMAP5, TIMM13
GO:0010740—positive regulation of protein kinase cascade	5	.049933	LIF, MAP3K7, TNFRSF1A, ATP2C1, EDA2R
GO:0044429—mitochondrial part	10	.043116	BID, SQORDL, NDUFS4, GIMAP5, CYP11A1, OGDHL, PITRM1, CARS2, TIMM13, POLG2
GO:0005520—insulin-like growth factor binding	4	.001127	NOV, WISP3, IGFBP6, IGFBP5
GO:0005509—calcium ion binding	16	.008952	CRELD1, MYL2, NELL2, S100A9, PCDH12, PCDHB12, MMP11, ASGR1, CHRNA9, ATP2C1, GRIN2D, RGN, B4GALT6, AOC2, PLCB2, RCN2
GO:0042803—protein homodimerization activity	8	.021388	ASGR1, TP53I3, PDXK, PYGL, EPHX2, MYH7, STK4, MTUS2
GO:0008378—galactosyltransferase activity	3	.032355	B3GNT3, UGT8, B4GALT6
GO:0031994—insulin-like growth factor I binding	2	.048894	IGFBP6, IGFBP5
hsa05014: Amyotrophic lateral sclerosis (ALS)	4	.010479	BID, TNFRSF1A, GRIA2, GRIN2D
hsa04260: Cardiac muscle contraction	4	.029315	FXYD2, MYL2, ATP1B3, MYH7

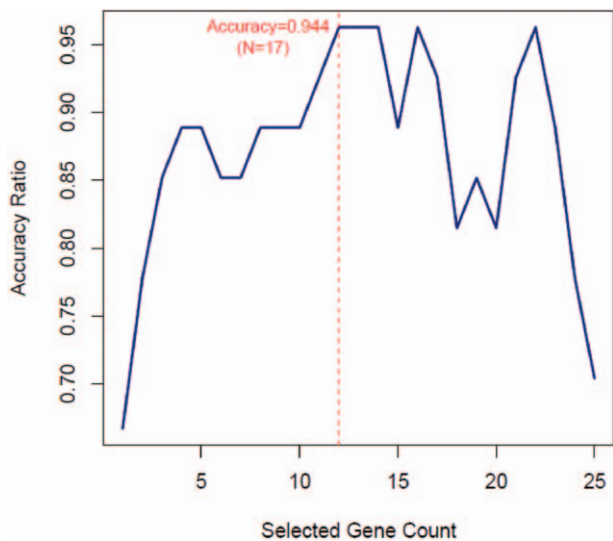


Figure 8. The optimal characterized genes combination selection by recursive feature elimination. The X-axis presents the number of selected characters. The Y-axis presents prediction accuracy of characters set.

Table 3
The optimal characterized genes combination list.

Genes	P	FDR	logFC
EDA2R	.00015	0.000956	-1.23302
MAP3K7	.00047	0.002994	1.038127
MMP11	.005422	0.034548	1.097573
LOC220077	.005556	0.035405	1.386148
CEP63	.005685	0.036224	1.055381
ATP2C1	.006793	0.043285	1.03876
CCPG1	.008203	0.042273	1.053882
IL17RC	.008464	0.043936	1.105048
LRRTM4	.008489	0.044094	-1.1295
MAFF	.011573	0.023742	-1.10561
FXYD2	.011649	0.024231	1.149089
CRELD1	.014441	0.04202	1.042934

FDR=false discovery rate, logFC=log (fold change).

combination. In GSE14827, SVM can classify 26 samples with accuracy rate of 96.3%. In GSE32981 and GSE21257, the classified samples were 22 and 48 with accuracy rate of 95.7% and 92.3%, respectively. The sample recognition and classification effect was synthetically determined according to Se, Sp, PPV, NPV, and areas under ROC curve (Fig. 9). The analysis results of SVM evaluation index were shown in Table 4.

4. Discussion

OS is the most common primary malignant bone tumor, which especially displays highly aggressive and early systemic metastasis in people at young age.^[1,2] More knowledge about the mechanism of OS metastasis is required for OS early diagnosis and treatment. In this study, we identified 897 DEGs. With the usage of WGCNA approach, 142 genes highly related with OS metastasis were obtained. These genes were enriched in cell growth regulation and insulin-like growth factor binding

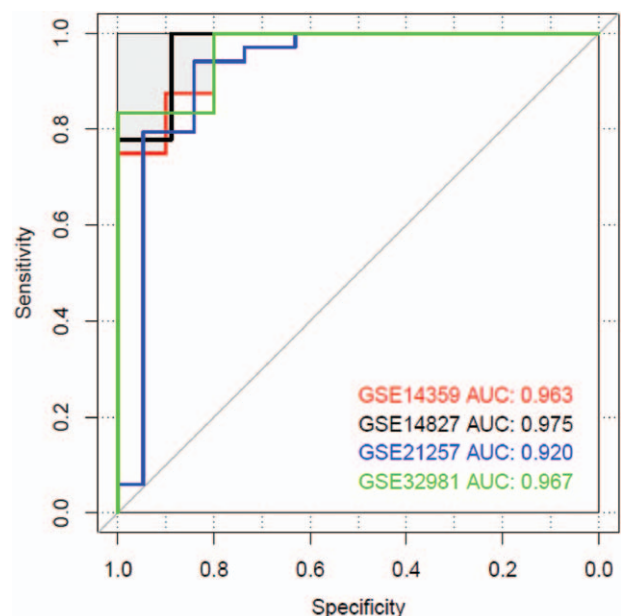


Figure 9. Area under the curve of ROC diagram of support vector machine.

Table 4**List of support vector machines (SVM) evaluation index in training datasets and test datasets.**

Datasets	Number of samples	Correct rate	Sensitivity	Specificity	PPV	NPV	AUROC
GSE14359	18	0.944	0.875	1	1	0.909	0.963
GSE14827	27	0.963	0.889	1	1	0.947	0.975
GSE21257	52	0.923	1	0.778	0.895	1	0.92
GSE32981	23	0.957	1	0.8	0.933	1	0.967

AUROC=area under the curve of ROC, NPV=negative predictive value, PPV=positive predictive value, SVM=support vector machine.

associated GO functions and KEGG pathways. Finally, considered GSE14359 as training dataset and conducted following RFE, we obtained 12 optimal characterized genes including FXYD2 and MMP11. SVM was further verified with the usage of the other 3 GSE14827, GSE21257, and GSE32981 datasets.

In this study, the selected 142 DEGs had been classified into several classical pathways (Table 2). Insulin-like growth factor binding proteins (IGFBPs) members can both positively or negatively regulate IGFs function.^[24,25] Among these IGFBPs members, IGFBP6 expression level was increased in OS metastasis group (Fig. 6). IGFBP-6 was able to inhibit actions of IGF-II, including IGF-II induced cell proliferation and differentiation by typical IGF-dependent pathway.^[26] However, recently studies showed that IGFBP6 can also promote cancer cell migration through IGF-independent manner, which may be transduced by mitogen-activated protein kinase (MAPK).^[27] WISP3, also named as CCN6, was another increased genes involved in insulin-like growth factor binding. WISP3 was regarded as one potential anti-cancer therapy target because it elicited OS cells metastasis by suppressing activation of TAK1 and p38.^[28] To our surprise, *IGFBP5*, one protein that inhibit tumorigenicity and metastasis of human osteosarcoma, also increased significantly in OS metastasis panel,^[29] which indicated the complexity of metastasis process.

In the 12 optimal characterized genes, *MMP11* has been detected in many invasive human carcinomas. In oral squamous cell carcinoma, *MMP11* expression level was associated with lymph node metastasis. Overexpression of *MMP11* in oral squamous cell carcinoma cells also promoted cell migration in vitro.^[30] In addition, another report indicated the potential role of *MMP11* existing in plasma in disease progression assessment, which suggested *MMP11* can be used as biomarker for diagnosis.^[31] FXYD domain Containing Ion Transport Regulator 2 (*FXYD2*) was the modulating subunit of Na⁺/K⁺-ATPases. In OCCC tissues, *FXYD2* significantly expressed. Deficiency of *FXYD2* led to tumor growth suppression, which indicated that *FXYD2* had the possibility to be antitumor target.^[32]

Although we identified DEGs between OS metastasis and non-metastasis through bioinformatics methods, we did not conduct experimental test for any of these selected genes, which was a limitation of this study. Functional analysis is necessary to further study the functions of these genes in OS metastasis progress regulation.

In conclusion, *IGFBP5*, *IGFBP6*, *WISP3*, and *MYL2* were involved in Insulin-like growth factor binding. This correlation gave us hypothesis that insulin-like growth factor binding associated genes may play important role in deciding OS metastasis progression. More basic functional experiments need to be conducted to investigate these involved genes function to explore more anti-tumor and metastasis inhibition targets.

Author contributions

Conceptualization: Honglai Tian, Donghui Guan, Jianmin Li.

Data curation: Honglai Tian, Donghui Guan.

Formal analysis: Jianmin Li.

Writing – original draft: Honglai Tian, Donghui Guan.

Writing – review & editing: Honglai Tian, Jianmin Li.

References

- Mirabello L, Troisi RJ, Savage SA. International osteosarcoma incidence patterns in children and adolescents, middle ages and elderly persons. *Int J Cancer* 2009;125:229–34.
- PJ M, RM G, FW A-K, et al. Osteosarcoma. *J Am Acad Orthop Surgeons* 2009;17:515.
- Eilber F, Giuliano A, Eckardt J, et al. Adjuvant chemotherapy for osteosarcoma: a randomized prospective trial. *J Clin Oncol* 1987;5:21–6.
- Allison DC, Carney SC, Ahlmann ER, et al. A meta-analysis of osteosarcoma outcomes in the modern medical era. *Sarcoma* 2012;2012:704872.
- Meyers PA, Heller G, Healey JH, et al. Osteogenic sarcoma with clinically detectable metastasis at initial presentation. *J Clin Oncol* 1993;11:449–53.
- Chou A, Merola P, Lh , et al. Treatment of osteosarcoma at first recurrence after contemporary therapy: the Memorial Sloan-Kettering Cancer Center experience. *Cancer* 2005;104:2214–21.
- Han G, Wang Y, Bi W. C-Myc overexpression promotes osteosarcoma cell invasion via activation of MEK-ERK pathway. *Oncol Res* 2012;20:149–56.
- Muff R, Ram Kumar RM, Botter SM, et al. Genes regulated in metastatic osteosarcoma: evaluation by microarray analysis in four human and two mouse cell line systems. *Sarcoma* 2012;2012:937506.
- Steeg PS, Bevilacqua G, Kopper L, et al. Evidence for a novel gene associated with low tumor metastatic potential. *J Natl Cancer Inst* 1988;80:200–4.
- Silva G, Aboussekhra A. p16 (INK4A) inhibits the pro-metastatic potentials of osteosarcoma cells through targeting the ERK pathway and TGF-beta1. *Mol Carcinog* 2016;55:525–36.
- Dong JT, Lamb PW, Rinker-Schaeffer CW, et al. KAI1, a metastasis suppressor gene for prostate cancer on human chromosome 11p11.2. *Science* 1995;268:884–6.
- Zhang Y, Tang YJ, Li ZH, et al. KiSS1 inhibits growth and invasion of osteosarcoma cells through inhibition of the MAPK pathway. *Eur J Histochem* 2013;57:e30.
- Presson AP, Sobel EM, Papp JC, et al. Integrated weighted gene co-expression network analysis with an application to chronic fatigue syndrome. *BMC Syst Biol* 2008;2:95.
- Langfelder P, Horvath S. WGCNA: an R package for weighted correlation network analysis. *BMC Bioinformatics* 2008;9:559.
- Zhou Q, Su X, Jing G, et al. Meta-QC-chain: comprehensive and fast quality control method for metagenomic data. *Genomics, Proteomics Bioinformatic* 2014;12:52.
- Malki K, Tosto MG, Jumabhoy I, et al. Integrative mouse and human mRNA studies using WGCNA nominates novel candidate genes involved in the pathogenesis of major depressive disorder. *Pharmacogenomics* 2013;14:1979–90.
- Udyavar AR, Hoeksema MD, Clark JE, et al. Co-expression network analysis identifies Spleen Tyrosine Kinase (SYK) as a candidate oncogenic driver in a subset of small-cell lung cancer. *BMC Syst Biol* 2013;7:S1.
- Liu X, Hu AX, Zhao JL, et al. Identification of Key Gene Modules for in Human Osteosarcoma by Co-expression Analysis weighted gene

- coexpression network analysis (WGCNA). *J Cell Biochem* 2017;118:3953.
- [19] Namlos HM, Kresse SH, Muller CR, et al. Global gene expression profiling of human osteosarcomas reveals metastasis-associated chemokine pattern. *Sarcoma* 2012;2012:639038.
- [20] Buddingh EP, Kuijjer ML, Duim RA, et al. Tumor-infiltrating macrophages are associated with metastasis suppression in high-grade osteosarcoma: a rationale for treatment with macrophage activating agents. *Clin Cancer Res* 2011;17:2110–9.
- [21] Kobayashi E, Masuda M, Nakayama R, et al. Reduced argininosuccinate synthetase is a predictive biomarker for the development of pulmonary metastasis in patients with osteosarcoma. *Mol Cancer Ther* 2010;9:535.
- [22] Liu WM, Mei R, Di X, et al. Analysis of high density expression microarrays with signed-rank call algorithms. *Bioinformatics* 2002;18:1593–9.
- [23] Gentleman R, Carey V, Huber W, et al. *Bioinformatics and Computational Biology Solutions Using R and Bioconductor* (Statistics for Biology and Health). Springer-Verlag, New York:2005.
- [24] Kelley KM, Oh Y, Gargosky SE, et al. Insulin-like growth factor-binding proteins (IGFBPs) and their regulatory dynamics. *Int J Biochem Cell Biol* 1996;28:619–37.
- [25] Collett-Solberg PF, Cohen P. The role of the insulin-like growth factor binding proteins and the IGFBP proteases in modulating IGF action. *Endocrinol Metab Clin North Am* 1996;25:591.
- [26] Bach LA. Insulin-like growth factor binding protein-6: The “forgotten” binding protein? *Horm Metab Res* 1999;31:226–34.
- [27] Bach LA, Fu P, Yang Z. Insulin-like growth factor-binding protein-6 and cancer. *Clin Sci* 2013;124:215–29.
- [28] Pal A, Huang W, Li X, et al. CCN6 modulates BMP signaling via the Smad-independent TAK1/p38 pathway, acting to suppress metastasis of breast cancer. *Cancer Res* 2012;72:4818.
- [29] Luther GA, Lamplot J, Chen X, et al. IGFBP5 domains exert distinct inhibitory effects on the tumorigenicity and metastasis of human osteosarcoma. *Cancer Lett* 2013;336:222–30.
- [30] Hsin CH, Chou YE, Yang SF, et al. MMP-11 promoted the oral cancer migration and Fak/Src activation. *Oncotarget* 2017;8:32783–93.
- [31] Hsin CH, Chen MK, Tang CH, et al. High level of plasma matrix metalloproteinase-11 is associated with clinicopathological characteristics in patients with oral squamous cell carcinoma 2014;9:e113129.
- [32] Hsu IL, Chou CY, Wu YY, et al. Targeting FXYD2 by cardiac glycosides potently blocks tumor growth in ovarian clear cell carcinoma. *Oncotarget* 2016;7:62925–38.